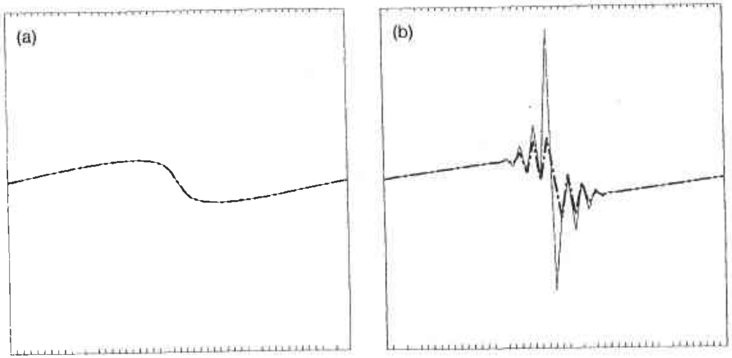

FIGURE 3.13. Differential–difference solution to Burgers's equation at (a) $t = 0.13$ and (b) $t = 0.28$ obtained using the advective form ((3.115), thin solid line) and the conservative form ((3.120) dot-dashed line).

and approximating this with the differential–difference equation

$$\frac{d\phi_j}{dt} + \frac{1}{2}\left(\frac{\phi_{j+1}^2 - \phi_{j-1}^2}{2\Delta x}\right) = 0. \tag{3.118}$$

Multiplying the preceding by ϕ_j and summing over the periodic domain yields

$$\frac{d}{dt}\sum_j \phi_j^2 = -\frac{1}{2}\sum_j \phi_j\phi_{j+1}\left(\frac{\phi_{j+1} - \phi_j)}{\Delta x}\right), \tag{3.119}$$

which demonstrates that the flux form also fails to conserve $\|\phi\|_2$. Since the terms representing the nonconservative forcing in (3.117) and (3.119) differ only by a factor of $-\frac{1}{2}$, it is possible to obtain a scheme that does conserve $\|\phi\|_2$ using a weighted average of the advective- and flux-form schemes. The resulting "conservative form" is

$$\frac{d\phi_j}{dt} + \frac{1}{3}\phi_j\left(\frac{\phi_{j+1} - \phi_{j-1}}{2\Delta x}\right) + \frac{1}{3}\left(\frac{\phi_{j+1}^2 - \phi_{j-1}^2}{2\Delta x}\right) = 0. \tag{3.120}$$

Figure 3.13 shows a comparison of the solutions to (3.115) and (3.120). The test problem is the same test considered previously in connection with Fig. 3.12, except that the vertical scale of the plotting domain shown in Fig. 3.13 has been reduced, and the second panel now shows solutions at $t = 0.28$. The unstable growth of the short-wavelength oscillations generated by advective-form differencing can be observed by comparing the solution at $t = 0.22$ (Fig. 3.12b) and $t = 0.28$ (Fig. 3.13b). As illustrated in Fig. 3.13b, short-wavelength oscillations

also develop in the conservative-form solution, but these oscillations do not continue to amplify.[8] The flux form (3.118) yields a solution (not shown) to this test problem that looks qualitatively similar to the conservative-form solution shown in Fig. 3.13b, although the spurious oscillations in the flux-form result are actually somewhat weaker. It is perhaps surprising that the short-wavelength oscillations are smaller in the flux-form solution than in the conservative-form solution and that the flux-form solution does not show a tendency toward instability. In fact, practical experience suggests that the flux-form difference (3.118) is not particularly susceptible to nonlinear instability. Fornberg (1973) has, nevertheless, demonstrated that both the advective and flux forms are unstable (and that the conservative form is stable) when the discretized initial condition has the special form $\ldots, 0, -1, 1, 0, -1, 1, 0, \ldots$.

The instabilities that develop in the preceding solutions to Burgers's equation appear to be associated with the formation of the shock. The development of a shock is not, however, a prerequisite for the onset of nonlinear instability, and such instabilities may occur in numerical simulations of very smooth flow. One example in which nonlinear instability develops in a smooth flow is provided by the viscous Burgers's equation

$$\frac{\partial\psi}{\partial t} + \psi\frac{\partial\psi}{\partial x} = \nu\frac{\partial^2\psi}{\partial x^2}, \tag{3.121}$$

where ν is a coefficient of viscosity. The true solution to the viscous Burgers's equation never develops a shock, but the advective-form differential difference approximation to (3.121) becomes unstable for sufficiently small values of ν.

3.6.2 *The Barotropic Vorticity Equation*

A second example involving the development of nonlinear instability in very smooth flow is provided by the equation governing the vorticity in a two-dimensional incompressible homogeneous fluid,

$$\frac{\partial\zeta}{\partial t} + \mathbf{u}\cdot\nabla\zeta = 0. \tag{3.122}$$

Here $\mathbf{u}$ is the two-dimensional velocity vector describing the flow in the x-y plane and ζ is the vorticity component along the z-axis. Since the flow is nondivergent, $\mathbf{u}$ and ζ may be expressed in terms of a stream function ψ such that

$$\mathbf{u} = \mathbf{k}\times\nabla\psi, \qquad \zeta = \mathbf{k}\cdot\nabla\times\mathbf{u} = \nabla^2\psi,$$

[8] Even though they do not lead to instability, the short-wavelength oscillations in the conservative-form solution to Burgers's equation are nonphysical and are not present in the correct generalized solution to Burgers's equation, which satisfies the Rankine–Hugoniot condition (5.10) at the shock and is smooth away from the shock. After the formation of the shock the correct generalized solution ceases to conserve $\|\phi\|^2$, so it can no longer be well-approximated by the numerical solution obtained using the conservative-form difference. In order to obtain good numerical approximations to discontinuous solutions to Burgers's equation it is necessary to use the methods discussed in Chapter 5

and (3.122) may be written as

$$\frac{\partial \nabla^2 \psi}{\partial t} + J(\psi, \nabla^2 \psi) = 0, \tag{3.123}$$

where J is the Jacobian operator

$$J(p, q) = \frac{\partial p}{\partial x}\frac{\partial q}{\partial y} - \frac{\partial p}{\partial y}\frac{\partial q}{\partial x}.$$

In atmospheric science, (3.123) is known as the barotropic vorticity equation.

Fjørtoft (1953) demonstrated that if the initial conditions are smooth, solutions to (3.123) must remain smooth in the sense that there can be no net transfer of energy from the larger spatial scales into the smaller scales. Fjørtoft's conclusions follow from the properties of the domain integral of the Jacobian operator. Let $\overline{p}$ denote the domain integral of p, and suppose, for simplicity, that the domain is periodic in x and y. Then by the assumed periodicity of the spatial domain[9]

$$\overline{J(p, q)} = \overline{\frac{\partial}{\partial x}\left(p\frac{\partial q}{\partial y}\right)} - \overline{\frac{\partial}{\partial y}\left(p\frac{\partial q}{\partial x}\right)} = 0.$$

As a consequence,

$$\overline{pJ(p, q)} = \overline{J(p^2/2, q)} = 0, \tag{3.124}$$

and

$$\overline{qJ(p, q)} = \overline{J(p, q^2/2)} = 0. \tag{3.125}$$

The preceding relations may be used to demonstrate that the domain-integrated kinetic energy and the domain-integrated enstrophy (one-half the vorticity squared) are both conserved. First consider the enstrophy, $\zeta^2/2 = (\nabla^2\psi)^2/2$. Multiplying (3.123) by $\nabla^2\psi$ and integrating over the spatial domain yields

$$\frac{\partial}{\partial t}\left(\frac{\overline{(\nabla^2\psi)^2}}{2}\right) + \overline{(\nabla^2\psi)J(\psi, \nabla^2\psi)} = 0,$$

which using (3.125) reduces to

$$\frac{\partial}{\partial t}\left(\frac{\overline{(\nabla^2\psi)^2}}{2}\right) = 0.$$

The conservation of the domain-integrated kinetic energy, $\mathbf{u}\cdot\mathbf{u}/2 = \nabla\psi\cdot\nabla\psi/2$, may be demonstrated by first noting that the vector identity

$$\nabla\cdot(\alpha\mathbf{a}) = \nabla\alpha\cdot\mathbf{a} + \alpha(\nabla\cdot\mathbf{a})$$

[9] Equivalent conservation properties hold in a rectangular domain in which the normal velocity is zero at all points along the boundary.

implies that

$$\psi\frac{\partial \nabla^2\psi}{\partial t} = \nabla\cdot\left(\psi\frac{\partial\nabla\psi}{\partial t}\right) - \frac{\partial}{\partial t}\left(\frac{\nabla\psi\cdot\nabla\psi}{2}\right).$$

Then multiplying (3.123) by ψ, using the preceding relation and integrating over the periodic spatial domain one obtains

$$\frac{\partial}{\partial t}\left(\frac{\overline{\nabla\psi\cdot\nabla\psi}}{2}\right) = 0.$$

Now suppose that the stream function is expanded in Fourier series along the x and y coordinates

$$\psi = \sum_k\sum_\ell a_{k,\ell}e^{i(kx+\ell y)} = \sum_{k,\ell}\psi_{k,\ell},$$

and define the total wave number κ such that $\kappa^2 = k^2 + \ell^2$. By the periodicity of the domain and the orthogonality of the Fourier modes,

$$\overline{\mathbf{u}\cdot\mathbf{u}} = \overline{\nabla\psi\cdot\nabla\psi} = \overline{\nabla\cdot(\psi\nabla\psi)} - \overline{\psi\nabla^2\psi} = -\overline{\psi\nabla^2\psi} = \sum_{k,\ell}\kappa^2\overline{\psi_{k,\ell}^2}$$

and

$$\overline{\zeta^2} = \overline{(\nabla^2\psi)^2} = \sum_{k,\ell}\kappa^4\overline{\psi_{k,\ell}^2}.$$

The two preceding relations may be used to evaluate an average wave number, κ_{avg}, given by the square root of the ratio of the domain-integrated enstrophy to the domain-integrated kinetic energy,

$$\kappa_{\text{avg}} = \left(\frac{\overline{\zeta^2}}{\overline{\mathbf{u}\cdot\mathbf{u}}}\right)^{1/2}.$$

Since the domain-integrated enstrophy and the domain-integrated kinetic energy are both conserved, κ_{avg} does not change with time. Any energy transfers that take place from larger to smaller scales must be accompanied by a second energy transfer from smaller to larger scales to conserve κ—there can be no systematic energy cascade into the short-wavelength components of the solution.

Suppose that the barotropic vorticity equation (3.123) is approximated using centered second-order differences in space and time such that

$$\delta_{2t}(\tilde{\nabla}^2\phi) + \tilde{J}(\phi, \tilde{\nabla}^2\phi) = 0,$$

where the numerical approximation to the horizontal Laplacian operator is

$$\tilde{\nabla}^2\phi = (\delta_x^2 + \delta_y^2)\phi$$

and the numerical approximation to the Jacobian operator is

$$\tilde{J}(p, q) = (\delta_{2x} p)(\delta_{2y} q) - (\delta_{2y} p)(\delta_{2x} q).$$

Phillips (1959) showed that solutions obtained using the preceding scheme are subject to an instability in which short-wavelength perturbations suddenly amplify without bound. This instability cannot be controlled by reducing the time step, and it occurs using values of Δt that are well below the threshold required to maintain the stability of equivalent numerical approximations to the linearized constant-coefficient problem. Phillips demonstrated that this instability could be controlled by removing all waves with wavelengths shorter than four grid intervals, thereby eliminating the possibility of aliasing error.

A more elegant method of stabilizing the solution was proposed by Arakawa (1966), who suggested reformulating the numerical approximation to the Jacobian to preserve the discrete analogue of the relations (3.124) and (3.125) and thereby obtain a numerical scheme that conserves both the domain-integrated enstrophy and kinetic energy. In particular, Arakawa proposed the following approximation to the Jacobian:

$$\begin{aligned}\tilde{J}_a(p, q) = {} & \frac{1}{3}\left[(\delta_{2x} p)(\delta_{2y} q) - (\delta_{2y} p)(\delta_{2x} q)\right] \\ & + \frac{1}{3}\left[\delta_{2x}(p\,\delta_{2y} q) - \delta_{2y}(p\,\delta_{2x} q)\right] + \frac{1}{3}\left[\delta_{2y}(q\,\delta_{2x} p) - \delta_{2x}(q\,\delta_{2y} p)\right].\end{aligned}$$

The Arakawa Jacobian satisfies the numerical analogue of (3.124) and (3.125),

$$\sum_{m,n} p_{m,n}\, \tilde{J}_a(p_{m,n}, q_{m,n}) = \sum_{m,n} q_{m,n}\, \tilde{J}_a(p_{m,n}, q_{m,n}) = 0, \tag{3.126}$$

where the summation is taken over all grid points in the computational domain. As a consequence of (3.126), solutions to

$$\frac{\partial}{\partial t}\left(\tilde{\nabla}^2 \phi\right) + \tilde{J}_a(\phi, \tilde{\nabla}^2 \phi) = 0 \tag{3.127}$$

conserve their domain-integrated enstrophy and kinetic energy and must therefore also conserve the discretized equivalent of the average wave number κ_{avg}. Since the average wave number is conserved, there can be no net amplification of the short-wavelength components in the numerical solution. The numerical solution is not only stable, it remains smooth.

Any numerical approximation to the barotropic vorticity equation will be stable if it conserves the domain-integrated kinetic energy, since that is equivalent to the conservation of $\|\mathbf{u}\|_2$. The enstrophy conservation property of the Arakawa Jacobian does more, however, than guarantee stability; it prevents a systematic cascade of energy into the shortest waves resolvable on the discrete mesh. In designing a numerical approximation to the barotropic vorticity equation it is clearly appropriate to chose a finite-difference scheme like the Arakawa Jacobian that inhibits the down-scale cascade of energy. On the other hand, it is not clear that schemes that limit the cascade of energy to small scales are appropriate in those fluid-dynamical applications where there actually is a systematic transfer of kinetic energy from large to small scale. Indeed, any accurate numerical approximation to the equations governing such flows must replicate this down-scale energy transfer.

One natural approach to the elimination of nonlinear instability in systems that support a down-scale energy cascade is through the parametrization of unresolved turbulent dissipation. In high-Reynolds-number (nearly inviscid) flow, kinetic energy is ultimately transferred to very small scales before being converted to internal energy by viscous dissipation, yet the storage limitations of digital computers do not allow most numerical simulations to be conducted with sufficient spatial resolution to resolve all the small-scale eddies involved in this energy cascade. Under such circumstances the kinetic energy transferred down-scale during the numerical simulation will tend to accumulate in the smallest scales resolvable on the numerical mesh, and it is generally necessary to remove this energy by some type of scale-selective dissipation. The scale-selective dissipation constitutes a parametrization of the influence of the unresolved eddies on the resolved-scale flow and should be designed to represent the true behavior of the physical system as closely as possible. Regardless of the exact formulation of the energy removal scheme, it will tend to stabilize the solution and prevent nonlinear instability.

Many fluid flows contain limited regions of active small-scale turbulence and relatively larger patches of dynamically stable laminar flow. Since eddy diffusion will not be active outside the regions of parametrized turbulence, a scale-selective background dissipation, similar to Phillips's (1959) technique of removing all wavelengths shorter than four grid intervals, is often required in order to avoid nonlinear instability. This dissipation may be implicitly included in the time-differencing or in an upwind-biased spatial difference, or it may be explicitly added to an otherwise nondamping method using formulae such as those discussed in Section 2.4.3. Although it is not required for stability, a small amount of background dissipation may also be incorporated in numerical approximations to linear partial differential equations to damp those short-wavelength components of the numerical solution whose phase speed and group velocity are most seriously in error.

Problems

1. Verify that the leapfrog time-differenced shallow-water equations (3.14) and (3.15) support a computational mode, and that the forward-backward-differenced system (3.17) and (3.18) does not, by solving their respective discrete-dispersion relations for ω.

2. Eliminate h from the finite-difference equations for the leapfrog unstaggered scheme (3.14) and (3.15) and compare the resulting higher-order finite-difference approximation to the second-order PDE